

Supplementary Materials to “Functional Regression Control Chart”

Fabio Centofanti¹, Antonio Lepore¹, Alessandra Menafoglio², Biagio Palumbo^{*1}, and Simone Vantini²

¹*Department of Industrial Engineering, University of Naples Federico II, Piazzale Tecchio 80, 80125, Naples, Italy*

²*MOX - Modelling and Scientific Computing, Department of Mathematics, Politecnico di Milano, Piazza Leonardo da Vinci 32, 20133, Milan, Italy*

technometrics tex template (do not remove)

*Corresponding author. e-mail: biagio.palumbo@unina.it

Table 1. Correlation functions and parameters for data generation in the simulation study.

Type		ρ	ν
Bessel	$J_\nu(z) = \left(\frac{ z /\rho^1}{2}\right)^\nu \sum_{j=0}^{\infty} \frac{(- z /\rho)^{2j/4}}{j!\Gamma(\nu+j+1)}$	0.25	0
Gaussian	$G(z) = \exp\left[-\left(\frac{ z }{\rho}\right)^2\right]$	1	-
Powered exponential	$P(z) = \exp\left[-\left(\frac{ z }{\rho}\right)^\nu\right]$	1	0.5

A Details on Data Generation

The compact domains \mathcal{S} and \mathcal{T} are set, without loss of generality, equal to $[0, 1]$ and the number of covariates p is set equal to 3. The eigenfunctions sets $\{\psi_i^X\}$ and $\{\psi_i^Y\}$ are generated by the spectral decomposition of pre-specified correlation functions. In particular, the eigenfunction set $\{\psi_i^X\}$ is obtained considering the correlation function \mathbf{G}^X through the following steps.

1. Set the diagonal elements G_{ll}^X , $l = 1, 2, 3$ of \mathbf{G}^X as the *Bessel* correlation function of the first kind (Abramowitz and Stegun, 1964), the *gaussian* correlation function (Abrahamsen and Regnesentral, 1997) and the *powered exponential* correlation function (Stein, 1999). The general form of the correlation functions and parameters used in the simulation study are listed in Table 1. Then, calculate the eigenvalues $\{\eta_{lk}^X\}$ and the corresponding eigenfunctions $\{\vartheta_{lk}^X\}$, $k = 1, 2, \dots$, of G_{ll}^X , $l = 1, 2, 3$.
2. Obtain the cross-correlation function G_{lj}^X , $l, j = 1, 2, 3$ and $l \neq j$, by

$$G_{lj}^X(s_1, s_2) = \sum_{k=1}^{\infty} \tilde{\eta}_k^X \tilde{\vartheta}_{lk}^X(s_1) \tilde{\vartheta}_{jk}^X(s_2) \quad s_1, s_2 \in \mathcal{S}, \quad (\text{A.1})$$

where $\tilde{\eta}_k^X = (1/3) \sum_{l=1}^3 \eta_{lk}^X$ and $\tilde{\vartheta}_{lk}^X = (1/\sqrt{3}) \vartheta_{lk}^X$.

3. Calculate the eigenvalues $\{\lambda_i^X\}$ and the corresponding eigenfunctions $\{\psi_i^X\}$ through the spectral decomposition of $\mathbf{G}^X = \{G_{lj}^X\}_{l,j=1,2,3}$, for $i = 1, \dots, L^*$.

The eigenvalues $\{\lambda_i^Y\}$ and the corresponding eigenfunctions $\{\psi_i^Y\}$, $i = 1, \dots, M^*$ are calculated by means of the spectral decomposition of G^Y set as the *Bessel correlation function*

Table 2. Diagonal values b_{ii} of \mathbf{B}_{LM11} and corresponding R^2 for three different settings.

b_{ii}	R^2
0.698, 0.838, 0.315, 0.0504, 0.002, 0.000, 0.000, 0.000, 0.000, 0.000	0.97
0.658, 0.795, 0.275, 0.010, 0.000, 0.000, 0.000, 0.000, 0.000, 0.000, 0.000	0.86
0.608, 0.745, 0.225, 0.000, 0.000, 0.000, 0.000, 0.000, 0.000, 0.000, 0.000	0.76

of the first kind with $\rho = 0.2$ and $\nu = 0$ (Abramowitz and Stegun, 1964). Further, set L^* and M^* equal to 50 and 10, respectively. Then, $\boldsymbol{\beta}$ is calculated as follows,

$$\boldsymbol{\beta}(s, t) = (\boldsymbol{\psi}^Y(t))^T (\mathbf{B}_{L^*M^*})^T \boldsymbol{\Psi}^X(s) \quad s, t \in [0, 1], \quad (\text{A.2})$$

where the matrix $\mathbf{B}_{L^*M^*}$, is set as a partitioned matrix $[\mathbf{B}_{L^*M^*11} \ \mathbf{B}_{L^*M^*21}]^T$, where $\mathbf{B}_{L^*M^*11}$ is a diagonal matrix of dimension M^* and $\mathbf{B}_{L^*M^*21}$ is a $(L^* - M^*) \times M^*$ matrix of all zeros. Diagonal values of $\mathbf{B}_{L^*M^*11}$ are listed in Table 2 for three different settings, along with the corresponding R^2 values (Horváth and Kokoszka, 2012; Yao et al., 2005), defined as

$$R^2 = \int_{[0,1]} \frac{\text{Var}(\mathbb{E}(Y(t) | \mathbf{X}))}{\text{Var}(Y(t))} dt. \quad (\text{A.3})$$

The R^2 value measures globally the proportion of the variance in the response explained by the covariates. Then, in order to ensure the validity of the model in Equation (3), $\boldsymbol{\Sigma}_{\boldsymbol{\epsilon}_{M^*}}$ is chosen such that the following relation holds

$$\boldsymbol{\Sigma}_{\boldsymbol{\xi}_{M^*}^Y} = \boldsymbol{\Lambda}^Y = (\mathbf{B}_{L^*M^*})^T \boldsymbol{\Lambda}^X \mathbf{B}_{L^*M^*} + \boldsymbol{\Sigma}_{\boldsymbol{\epsilon}_{M^*}}, \quad (\text{A.4})$$

with $\boldsymbol{\Sigma}_{\boldsymbol{\xi}_{M^*}^Y} = \text{Cov}(\boldsymbol{\xi}_{M^*}^Y)$, $\boldsymbol{\Lambda}^Y = \text{diag}(\lambda_1^Y, \dots, \lambda_{M^*}^Y)$, and $\boldsymbol{\Lambda}^X = \text{diag}(\lambda_1^X, \dots, \lambda_{L^*}^X)$. Realizations of \mathbf{X} are obtained through

$$\mathbf{X} = \sum_{i=1}^{L^*} \xi_i^X \boldsymbol{\psi}_i^X, \quad (\text{A.5})$$

with $\boldsymbol{\xi}_{L^*}^X = (\xi_1^X, \dots, \xi_{L^*}^X)^T$ generated by means of a multivariate normal distribution with covariance $\text{Cov}(\boldsymbol{\xi}_{L^*}^X) = \boldsymbol{\Sigma}_{\boldsymbol{\xi}_{L^*}^X} = \boldsymbol{\Lambda}^X$. In the same way, realizations of Y are generated by

Table 3. Values of m_i and s_i to generate the mean functions $\boldsymbol{\mu}^{\tilde{X}} = (\mu_1^{\tilde{X}}, \mu_2^{\tilde{X}}, \mu_3^{\tilde{X}})^T$ and $\mu^{\tilde{Y}}$, and the variance functions $\mathbf{v}^{\tilde{X}} = (v_1^{\tilde{X}}, v_2^{\tilde{X}}, v_3^{\tilde{X}})^T$ and $v^{\tilde{Y}}$ of $\tilde{\mathbf{X}}$ and \tilde{Y} , respectively, in the simulation study.

	m_i	s_i
$\mu_1^{\tilde{X}}$	0.075, 0.100, 0.250, 0.350, 0.500, 0.650, 0.850, 0.900, 0.950	0.050, 0.030, 0.050, 0.050, 0.100, 0.050, 0.100, 0.040, 0.035
$\mu_2^{\tilde{X}}$	-	-
$\mu_3^{\tilde{X}}$	0.075, 0.100, 0.150, 0.225, 0.400, 0.525, 0.550, 0.600, 0.625, 0.650, 0.850, 0.900, 0.925	0.050, 0.060, 0.050, 0.040, 0.050, 0.035, 0.045, 0.045, 0.040, 0.030, 0.015, 0.010, 0.015
$\mu^{\tilde{Y}}$	-	-
$v_1^{\tilde{X}}$	0.075, 0.100, 0.125, 0.150, 0.400, 0.650, 0.850, 0.900, 0.925	0.050, 0.060, 0.075, 0.075, 0.075, 0.045, 0.045, 0.040
$v_2^{\tilde{X}}$	-	-
$v_3^{\tilde{X}}$	0.075, 0.100, 0.150, 0.225, 0.400, 0.525, 0.550, 0.600, 0.625, 0.650, 0.850, 0.900, 0.925	0.050, 0.060, 0.050, 0.040, 0.050, 0.035, 0.045, 0.045, 0.040, 0.030, 0.015, 0.010, 0.015
$v^{\tilde{Y}}$	-	-

means of

$$Y = \sum_{i=1}^{M^*} \xi_i^Y \boldsymbol{\psi}_i^Y. \quad (\text{A.6})$$

Realizations of the score vector $\boldsymbol{\xi}_{M^*}^Y = (\xi_1^Y, \dots, \xi_{M^*}^Y)^T$ are obtained as

$$\boldsymbol{\xi}_{M^*}^Y = (\mathbf{B}_{L^*M^*})^T \boldsymbol{\xi}_{L^*}^X + \boldsymbol{\epsilon}_{M^*}, \quad (\text{A.7})$$

with $\boldsymbol{\epsilon}_{M^*} = (\epsilon_1, \dots, \epsilon_{M^*})^T$ generated by means of a multivariate normal distribution with covariance matrix $\text{Cov}(\boldsymbol{\epsilon}_{M^*}) = \boldsymbol{\Sigma}_{\boldsymbol{\epsilon}_{M^*}}$ independent of $\boldsymbol{\xi}_{L^*}^X$. Further, the mean functions $\boldsymbol{\mu}^{\tilde{X}} = (\mu_1^{\tilde{X}}, \mu_2^{\tilde{X}}, \mu_3^{\tilde{X}})^T$ and $\mu^{\tilde{Y}}$ and the variance functions $\mathbf{v}^{\tilde{X}} = (v_1^{\tilde{X}}, v_2^{\tilde{X}}, v_3^{\tilde{X}})^T$ and $v^{\tilde{Y}}$ are generated through the following reference model

$$\mu(z) = P(z) + r \sum_{i=1}^I h_i(z; m_i, s_i) \quad z \in [0, 1], \quad (\text{A.8})$$

where

$$P(z) = az^2 + bz + c \quad z \in [0, 1], \quad (\text{A.9})$$

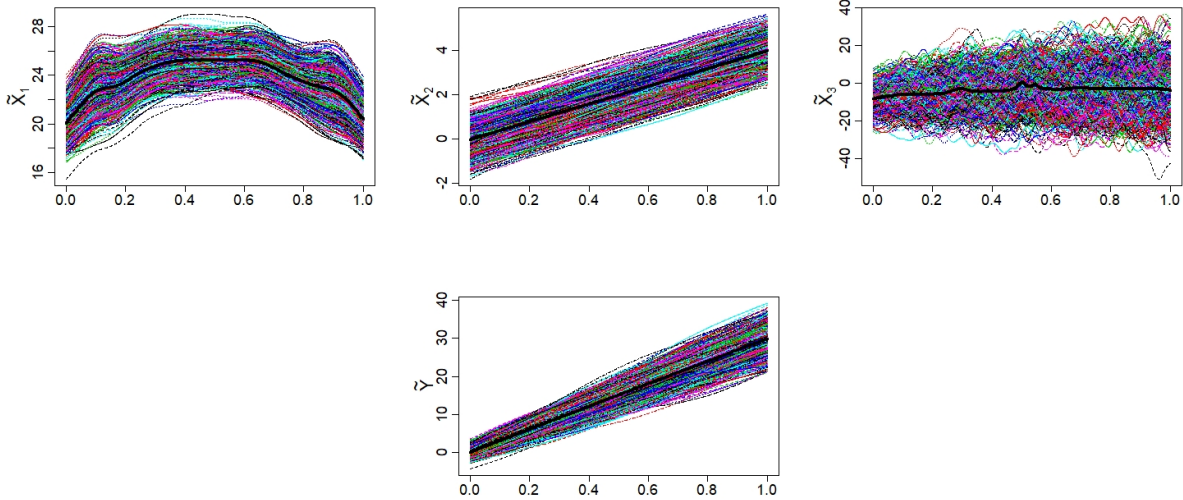
a , b , c are real numbers, the terms $h_i(z; m_i, s_i)$ are normal probability density functions having parameters m_i and s_i and z is equal to s (resp. t) if we are computing $\boldsymbol{\mu}^{\tilde{X}}$ (resp. $\mu^{\tilde{Y}}$). The values of all unknown parameters are listed in Table 3 and Table 4. Then, given the mean functions $\boldsymbol{\mu}^{\tilde{X}}$ and $\mu^{\tilde{Y}}$ and the variance functions $\mathbf{v}^{\tilde{X}}$ and $v^{\tilde{Y}}$, realizations of $\tilde{\mathbf{X}}$ and \tilde{Y} are easily obtained. Finally, $\tilde{\mathbf{X}}$ and \tilde{Y} are assumed to be observed at 150 equally

Table 4. Values of a , b , c and r to generate the mean functions $\boldsymbol{\mu}^{\tilde{X}} = (\mu_1^{\tilde{X}}, \mu_2^{\tilde{X}}, \mu_3^{\tilde{X}})^T$ and $\mu^{\tilde{Y}}$, and the variance functions $\mathbf{v}^{\tilde{X}} = (v_1^{\tilde{X}}, v_2^{\tilde{X}}, v_3^{\tilde{X}})^T$ and $v^{\tilde{Y}}$ of $\tilde{\mathbf{X}}$ and \tilde{Y} , respectively, in the simulation study.

	a	b	c	r
$\mu_1^{\tilde{X}}$	-20	20	-20	0.05
$\mu_2^{\tilde{X}}$	0	4	0	0
$\mu_3^{\tilde{X}}$	-10	14	-8	0.05
$\mu^{\tilde{Y}}$	0	30	0	0
$v_1^{\tilde{X}}$	0	0	1	0.1
$v_2^{\tilde{X}}$	0	0.02	1	0
$v_3^{\tilde{X}}$	-40	150	30	2
$v^{\tilde{Y}}$	0	8	1	0

spaced time points $[0, 1]$ with measurement errors $\zeta_i^{\tilde{X}} \sim N(\mathbf{0}, \boldsymbol{\sigma}_{\tilde{X}}^2)$ and $\zeta_i^{\tilde{Y}} \sim N(0, \sigma_{\tilde{Y}}^2)$ where $\boldsymbol{\sigma}_{\tilde{X}} = (0.3, 0.05, 0.3)^T$ and $\sigma_{\tilde{Y}} = 0.3$. For illustrative purposes, a sample of 1000 randomly generated realizations of $\tilde{\mathbf{X}} = (\tilde{X}_1, \tilde{X}_2, \tilde{X}_3)^T$ and \tilde{Y} with their mean functions are shown in Figure 1 for $R^2 = 0.97$.

Figure 1. 1000 randomly generated realizations of $\tilde{\mathbf{X}} = (\tilde{X}_1, \tilde{X}_2, \tilde{X}_3)^T$ and \tilde{Y} with their mean functions (black solid line).

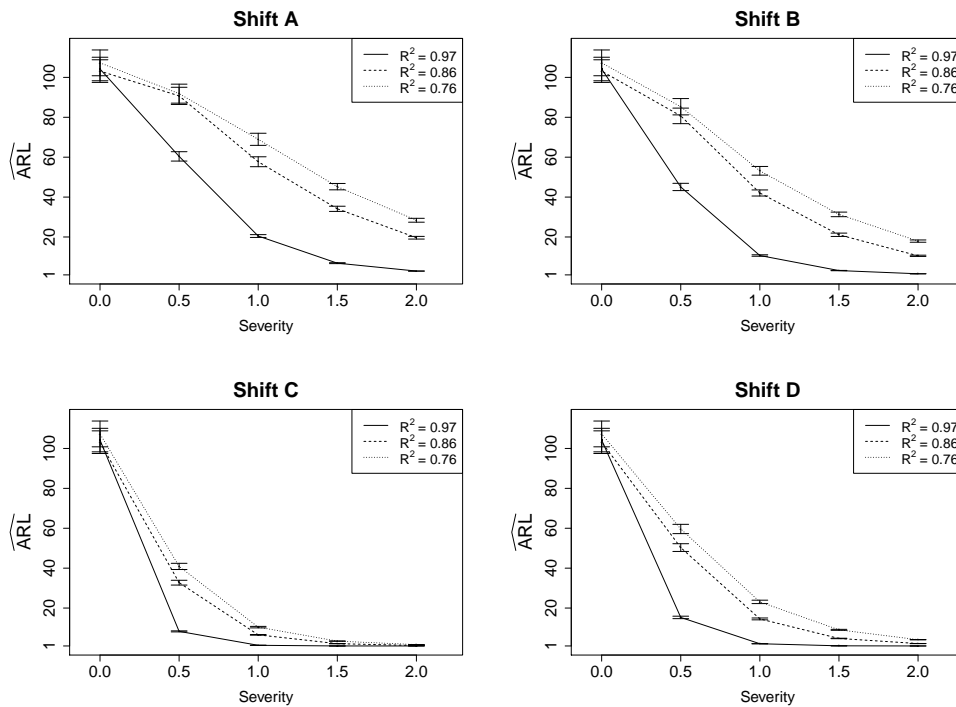


B FRCC Performance at Different Values of R^2

In the simulation study, the analysis were performed using data generated by considering diagonal values of $\mathbf{B}_{L^*M^*11}$ corresponding to $R^2 = 0.97$. To asses the effect on the FRCC

performance of changes in the proportion of the response variance explained by the covariates, the same analysis of Scenario 1 in Section 3.2 are performed by considering the three different settings in Table 2. As expected, when R^2 decreases, Figure 2 and Table 5 show that the FRCC advantage over its competitors becomes marginal, but the conclusions remain overall consistent with those taken in the case $R^2 = 0.97$. This confirms the fact that when no linear relation hold between the response and the covariates the FRCC and the RESP control chart perform equivalently. However, already at $R^2 = 0.76$ the FRCC performs better than the competitors control charts.

Figure 2. Estimated ARL (\widehat{ARL}) and 95% confidence interval achieved by FRCC at $R^2 = 0.76$ (dotted line), $R^2 = 0.86$ (dashed line) and $R^2 = 0.97$ (solid line), for each type of shift considered for Scenario 1 (Table 2a in the main document), as a function of the severity level.



C \widehat{ARL} s and 95% Approximate Confidence Intervals for Scenario 1 and Scenario 2 in the Simulation Study

Table 6 and Table 7 show the estimated ARLs for the the FRCC, RESP and INBA frameworks, for Scenario 1 and Scenario 2 based on the Student's t approximation. By looking at

Table 5. Estimated ARL ($\widehat{\text{ARL}}$) and 95% confidence interval achieved by FRCC, at $R^2 = 0.76, 0.86, 0.97$, for each type of shift and severity level considered for Scenario 1 (Table 2a in the main document).

Shift	Severity	R^2					
		0.97		0.86		0.76	
	d	$\widehat{\text{ARL}}$	CI	$\widehat{\text{ARL}}$	CI	$\widehat{\text{ARL}}$	CI
In-control	-	103.67	[98.56, 108.78]	103.42	[97.75, 109.08]	101.64	[96.20, 107.08]
A	0.5	60.40	[58.05, 62.75]	90.73	[86.43, 95.04]	91.85	[87.09, 96.61]
	1.0	20.48	[19.77, 21.18]	57.71	[55.23, 60.20]	68.96	[65.92, 72.00]
	1.5	6.88	[6.65, 7.11]	34.12	[32.82, 35.42]	45.23	[43.64, 46.83]
	2.0	2.91	[2.85, 2.97]	19.63	[18.96, 20.30]	28.38	[27.41, 29.36]
B	0.5	45.08	[43.26, 46.90]	80.70	[76.81, 84.60]	85.29	[81.20, 89.38]
	1.0	10.71	[10.34, 11.08]	42.06	[40.53, 43.58]	53.17	[50.99, 55.35]
	1.5	3.16	[3.09, 3.24]	21.10	[20.27, 21.94]	31.32	[30.18, 32.47]
	2.0	1.55	[1.53, 1.57]	10.56	[10.25, 10.88]	17.94	[17.37, 18.51]
C	0.5	8.31	[8.05, 8.57]	32.72	[31.53, 33.92]	40.87	[39.32, 42.43]
	1.0	1.33	[1.32, 1.34]	6.57	[6.40, 6.74]	10.43	[10.06, 10.81]
	1.5	1.00	[1.00, 1.00]	2.15	[2.11, 2.19]	3.43	[3.36, 3.50]
	2.0	1.00	[1.00, 1.00]	1.22	[1.21, 1.23]	1.67	[1.65, 1.70]
D	0.5	15.31	[14.69, 15.92]	50.31	[48.37, 52.25]	59.64	[57.32, 61.97]
	1.0	2.11	[2.08, 2.14]	14.56	[14.09, 15.02]	23.10	[22.24, 23.95]
	1.5	1.07	[1.07, 1.07]	4.76	[4.64, 4.87]	9.08	[8.84, 9.33]
	2.0	1.00	[1.00, 1.00]	2.20	[2.17, 2.24]	4.15	[4.05, 4.24]

the estimated ARLs achieved by the FRCC, we note that the Hotelling's T^2 control chart is more sensitive to mean shift than the SPE control chart, whereas, the two charts perform comparably for the RESP control chart. These results are also graphically displayed in Figure 1 and Figure 2 of the main document.

D FRCC Performance at Different Percentages of Variance Explained by Retained Principal Components

In this section, additional simulations are run for Scenario 1 (see Section 3) at each shift type and severity level reported in Table 1 and Table 2a of the main article, respectively, to study the effect on the FRCC performance of δ_Y and δ_X (i.e., percentage of total variance explained by the retained principal components in the response and covariates, respectively). Figure 3 displays the estimated ARL ($\widehat{\text{ARL}}$) and 95% confidence interval obtained from 100 simulation runs performed at $\delta_Y = 0.90, 0.95, 0.99$ and $\delta_X = 0.90, 0.95, 0.99$, for every shift type and severity level. It is clear from Figure 3 that, although the choice of δ_Y and δ_X may be case-specific and related to the bias-variance trade-off, δ_Y and δ_X larger

Table 6. Estimated ARL (\widehat{ARL}) and 95% confidence intervals (CI) achieved by FRCC, RESP and INBA along with estimated ARL for the Hotelling's T^2 (\widehat{ARL}_{T^2}) and SPE (\widehat{ARL}_{SPE}), achieved by FRCC and RESP, for each type of shift and severity level considered for Scenario 1 (Table 2a in the main document).

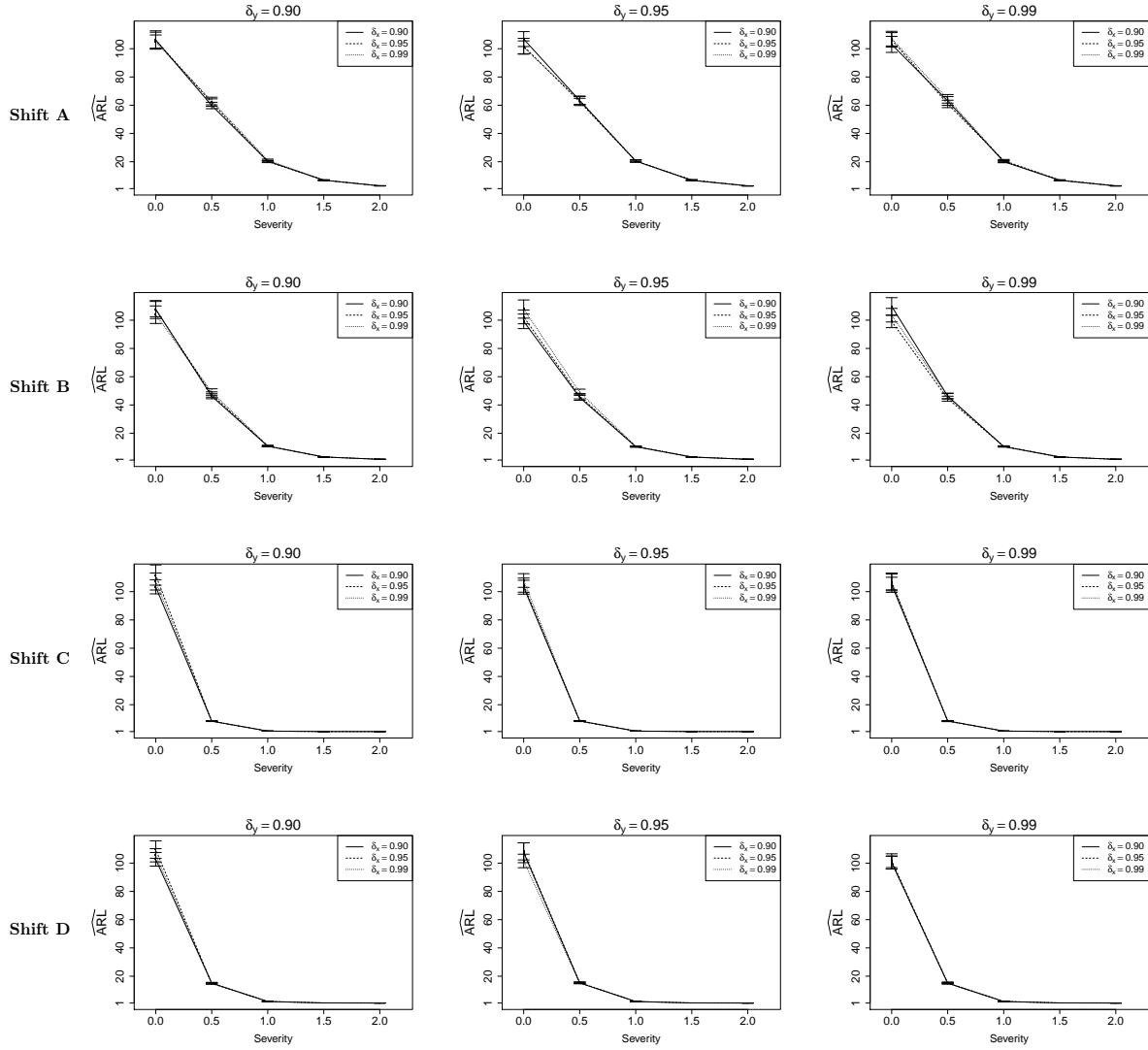
Shift	Severity	FRCC				RESP				INBA	
		d	\widehat{ARL}	CI	\widehat{ARL}_{T^2}	\widehat{ARL}_{SPE}	\widehat{ARL}	CI	\widehat{ARL}_{T^2}	\widehat{ARL}_{SPE}	\widehat{ARL}
In-control	-	103.67	[98.56, 108.78]	233.03	207.69	103.77	[98.99, 108.54]	231.03	211.09	104.00	[99.91, 108.09]
	0.50	60.40	[58.05, 62.75]	96.19	189.08	97.11	[91.74, 102.47]	219.52	201.26	101.80	[97.71, 105.90]
A	1.00	20.48	[19.77, 21.18]	23.83	160.03	86.25	[82.03, 90.48]	200.62	169.07	91.02	[87.69, 94.35]
	1.50	6.88	[6.65, 7.11]	7.33	108.82	70.22	[67.00, 73.45]	168.55	129.98	75.08	[72.91, 77.24]
	2.00	2.91	[2.85, 2.97]	3.00	74.64	54.57	[52.29, 56.85]	132.59	99.96	62.11	[60.10, 64.12]
	0.50	45.08	[43.26, 46.90]	63.19	177.38	97.44	[92.81, 102.07]	214.27	200.60	94.14	[90.53, 97.75]
B	1.00	10.71	[10.34, 11.08]	11.81	121.91	85.04	[80.81, 89.26]	179.90	179.47	73.87	[71.19, 76.54]
	1.50	3.16	[3.09, 3.24]	3.28	75.51	69.34	[66.07, 72.61]	134.86	157.78	57.57	[55.78, 59.35]
	2.00	1.55	[1.53, 1.57]	1.57	42.70	52.27	[50.21, 54.32]	97.63	121.31	40.64	[39.65, 41.64]
	0.50	8.31	[8.05, 8.57]	9.15	88.49	65.90	[63.32, 68.48]	168.19	117.69	77.22	[74.82, 79.61]
C	1.00	1.33	[1.32, 1.34]	1.35	24.29	25.31	[24.05, 26.56]	88.68	36.45	40.95	[39.86, 42.04]
	1.50	1.00	[1.00, 1.00]	1.01	7.97	10.60	[10.23, 10.97]	46.91	13.62	21.06	[20.58, 21.53]
	2.00	1.00	[1.00, 1.00]	1.00	3.56	5.09	[4.95, 5.23]	24.27	6.26	11.71	[11.51, 11.91]
D	0.50	15.31	[14.69, 15.92]	17.53	125.00	90.04	[85.03, 95.05]	202.77	180.29	84.18	[81.31, 87.04]
	1.00	2.11	[2.08, 2.14]	2.16	58.04	53.51	[51.55, 55.48]	114.75	107.90	49.06	[47.72, 50.40]
	1.50	1.07	[1.07, 1.07]	1.08	25.15	31.63	[30.54, 32.72]	66.51	63.04	28.27	[27.69, 28.85]
	2.00	1.00	[1.00, 1.00]	1.00	12.36	19.47	[18.82, 20.13]	41.71	37.49	16.87	[16.51, 17.23]

than 0.90 do not significantly affect the performance of the FRCC. In general, the larger the δ_Y and δ_X values, the less they affect the \widehat{ARL} .

Table 7. Estimated ARL (\widehat{ARL}) and 95% confidence intervals (CI) achieved by FRCC, RESP and INBA along with estimated ARL for the Hotelling's T^2 (\widehat{ARL}_{T^2}) and SPE (\widehat{ARL}_{SPE}), achieved by FRCC and RESP, for each type of shift and severity level considered for Scenario 2 (Table 2b in the main document). Zeros and ones in the triplets (000, 100, 010, 001, 110, 101, 011, 111) indicate IC and OC covariates, respectively. For instance, the triplet 100 means that only the first covariate is OC, 111 means that all the covariates are OC, and so on.

d	$\mu^{\bar{Y}}$	shifted covariate combination	FRCC				RESP				INBA	
			\widehat{ARL}	CI	\widehat{ARL}_{T^2}	\widehat{ARL}_{SPE}	\widehat{ARL}	CI	\widehat{ARL}_{T^2}	\widehat{ARL}_{SPE}	\widehat{ARL}	CI
0	0 0 0	103.68	[98.84, 108.52]	224.93	212.66	99.00	[94.43, 103.57]	205.19	209.90	102.62	[98.84, 106.40]	
	1 0 0	78.51	[74.41, 82.61]	230.90	128.03	88.94	[83.49, 94.39]	160.63	226.09	96.62	[92.42, 100.82]	
	0 1 0	98.06	[93.22, 102.90]	206.23	229.34	83.83	[80.01, 87.66]	160.32	207.11	81.15	[78.44, 83.85]	
	0 0 1	101.80	[96.58, 107.01]	231.09	206.50	105.04	[99.53, 110.55]	223.48	220.26	101.81	[97.58, 106.05]	
	1 1 0	75.47	[72.12, 78.83]	213.84	123.57	69.43	[66.38, 72.49]	109.66	208.60	98.37	[94.36, 102.37]	
	1 0 1	65.09	[62.55, 67.62]	223.88	95.74	98.95	[93.19, 104.72]	198.42	230.02	101.41	[97.46, 105.36]	
	0 1 1	98.80	[94.58, 103.02]	228.03	198.86	92.27	[87.91, 96.62]	176.01	219.36	78.71	[76.25, 81.16]	
	1 1 1	62.90	[60.04, 65.75]	215.26	94.17	75.49	[72.36, 78.62]	132.47	206.32	91.47	[88.31, 94.63]	
0.5	0 0 0	64.02	[60.79, 67.24]	100.56	199.58	97.87	[93.32, 102.43]	209.77	206.24	101.17	[97.87, 104.48]	
	1 0 0	43.51	[41.93, 45.08]	97.42	83.52	87.69	[83.46, 91.91]	169.52	202.96	87.15	[84.38, 89.93]	
	0 1 0	63.88	[60.93, 66.83]	103.42	184.81	98.35	[93.56, 103.15]	195.85	228.30	96.99	[93.76, 100.21]	
	0 0 1	60.92	[58.31, 63.53]	98.93	177.52	96.42	[91.48, 101.36]	197.20	218.29	100.12	[96.46, 103.78]	
	1 1 0	43.62	[41.96, 45.28]	94.14	86.66	74.22	[71.22, 77.22]	128.47	203.91	102.47	[98.62, 106.33]	
	1 0 1	39.96	[38.59, 41.34]	95.61	72.20	94.10	[89.60, 98.61]	182.32	222.00	90.46	[87.12, 93.80]	
	0 1 1	58.54	[56.10, 60.98]	94.93	172.01	98.01	[92.81, 103.21]	200.14	219.36	91.28	[87.73, 94.83]	
	1 1 1	39.29	[37.83, 40.76]	98.35	69.97	87.17	[82.97, 91.37]	159.95	215.91	102.34	[98.37, 106.31]	
1.0	0 0 0	20.72	[19.95, 21.49]	24.28	152.07	85.79	[81.97, 89.61]	192.98	169.13	87.50	[84.15, 90.86]	
	1 0 0	17.25	[16.61, 17.90]	24.81	59.50	79.12	[74.30, 83.93]	168.80	167.42	72.55	[69.85, 75.25]	
	0 1 0	21.37	[20.64, 22.10]	25.30	153.27	97.77	[94.29, 101.26]	220.36	200.63	102.43	[98.53, 106.33]	
	0 0 1	20.76	[19.99, 21.54]	25.54	119.09	82.14	[78.44, 85.83]	180.80	165.61	91.38	[88.03, 94.73]	
	1 1 0	17.39	[16.78, 17.99]	25.71	55.77	78.19	[74.48, 81.91]	139.34	202.44	102.21	[98.87, 105.55]	
	1 0 1	16.01	[15.48, 16.55]	24.52	47.49	81.09	[77.37, 84.81]	168.84	169.95	76.95	[73.87, 80.03]	
	0 1 1	20.64	[19.75, 21.53]	25.29	126.23	96.44	[91.94, 100.94]	209.49	199.31	99.53	[96.08, 102.98]	
	1 1 1	16.27	[15.83, 16.70]	25.22	46.88	88.79	[84.34, 93.24]	183.48	195.89	102.58	[98.72, 106.43]	
1.5	0 0 0	6.98	[6.76, 7.20]	7.48	104.42	71.01	[67.56, 74.47]	164.01	136.11	74.61	[72.17, 77.05]	
	1 0 0	6.16	[5.99, 6.33]	7.12	42.86	63.62	[60.46, 66.78]	133.23	129.84	60.13	[58.44, 61.83]	
	0 1 0	7.15	[6.94, 7.36]	7.65	107.79	88.23	[83.91, 92.54]	214.84	164.64	99.90	[96.09, 103.71]	
	0 0 1	6.94	[6.71, 7.17]	7.52	85.53	67.50	[64.45, 70.55]	152.58	133.78	79.45	[76.43, 82.47]	
	1 1 0	6.31	[6.15, 6.48]	7.30	42.89	77.27	[73.45, 81.10]	159.13	163.57	94.95	[91.36, 98.55]	
	1 0 1	6.18	[5.99, 6.38]	7.45	33.72	69.55	[66.63, 72.46]	160.59	130.90	63.93	[61.94, 65.92]	
	0 1 1	6.95	[6.72, 7.18]	7.58	81.18	88.47	[84.13, 92.81]	213.29	166.77	102.35	[98.39, 106.30]	
	1 1 1	6.40	[6.20, 6.61]	7.78	35.48	82.58	[78.31, 86.85]	188.38	166.13	93.41	[90.31, 96.50]	
2.0	0 0 0	2.94	[2.87, 3.01]	3.02	79.13	54.21	[51.68, 56.73]	135.63	96.71	62.89	[60.96, 64.82]	
	1 0 0	2.80	[2.74, 2.86]	3.02	28.77	54.69	[52.13, 57.25]	122.63	105.76	48.12	[46.78, 49.46]	
	0 1 0	2.96	[2.91, 3.02]	3.05	77.76	76.05	[72.17, 79.93]	208.91	129.36	97.19	[93.43, 100.96]	
	0 0 1	2.93	[2.86, 3.00]	3.05	56.38	52.56	[50.37, 54.76]	127.49	98.51	65.68	[63.25, 68.11]	
	1 1 0	2.81	[2.75, 2.86]	3.02	28.94	66.61	[63.52, 69.69]	156.75	126.63	79.18	[76.38, 81.97]	
	1 0 1	2.80	[2.74, 2.86]	3.06	24.63	53.00	[50.67, 55.34]	130.02	96.06	50.26	[48.68, 51.84]	
	0 1 1	2.97	[2.91, 3.02]	3.08	60.24	74.26	[71.00, 77.52]	209.91	124.02	94.70	[90.95, 98.45]	
	1 1 1	2.83	[2.77, 2.89]	3.10	23.86	70.22	[66.68, 73.76]	178.75	126.22	83.43	[79.98, 86.87]	

Figure 3. Estimated ARL (\widehat{ARL}) and 95% confidence interval achieved by FRCC for Scenario 1 (Table 2a in the main document), for each shift type (row-wise) and $\delta_Y = 0.90, 0.95, 0.99$ (column-wise, increasing from left to right panels), with $\delta_X = 0.90$ (solid line), 0.95 (dashed line), 0.99 (dotted line), as a function of the severity level.



E An Asymptotic Property of the Studentized Functional Residual

From Equation (34), it follows that the bias in the estimated residual e_Δ vanishes as the sample size and the truncation parameters increase. Here, we want to show that the same happens for the bias of the studentized residual $e_{stu\Delta}$ in presence of covariate mean shifts. Equation (35) defines e_{stu} in presence of covariate mean shifts for a new random observation

$(\mathbf{X}_\Delta, Y_\Delta)$ as

$$e_{stu\Delta}(t) = \frac{e_\Delta(t)}{\text{Cov}_{Y_\Delta, Y_i}(Y_\Delta - \hat{Y}_{LM} | \mathbf{X}_\Delta, \mathbf{X}_i)^{1/2}(t)} \quad t \in [0, 1].$$

Therefore, for $t \in [0, 1]$, the mean of $e_{stu\Delta}$ is

$$\mathbb{E}_{Y_\Delta, Y_i}(e_{stu\Delta} | \mathbf{X}_\Delta, \mathbf{X}_i)(t) = \mathbb{E}_{Y_i}[\mathbb{E}_{Y_\Delta}(e_{stu\Delta} | \mathbf{X}_\Delta, \mathbf{X}_i, Y_i) | \mathbf{X}_\Delta, \mathbf{X}_i](t),$$

where

$$\begin{aligned} & \mathbb{E}_{Y_\Delta}(e_{stu\Delta} | \mathbf{X}_\Delta, \mathbf{X}_i, Y_i)(t) \\ &= \mathbb{E}_{Y_\Delta} \left(\frac{e_\Delta}{\text{Cov}_{Y_\Delta, Y_i}(Y_\Delta - \hat{Y}_{LM} | \mathbf{X}_\Delta, \mathbf{X}_i)^{1/2} | \mathbf{X}_\Delta, \mathbf{X}_i, Y_i} \right) (t) \\ &= \frac{\mathbb{E}_{Y_\Delta}(e_\Delta | \mathbf{X}_\Delta, \mathbf{X}_i, Y_i)}{\text{Cov}_{Y_\Delta, Y_i}(Y_\Delta - \hat{Y}_{LM} | \mathbf{X}_\Delta, \mathbf{X}_i)^{1/2}(t)} \\ &= \frac{\int_0^1 (\boldsymbol{\beta}(s, t) - \hat{\boldsymbol{\beta}}_{LM}(s, t))^T \mathbf{V}^{\tilde{\mathbf{X}}}(s)^{-1} \boldsymbol{\Delta}^{\tilde{\mathbf{X}}}(s) ds}{\text{Cov}_{Y_\Delta, Y_i}(Y_\Delta - \hat{Y}_{LM} | \mathbf{X}_\Delta, \mathbf{X}_i)^{1/2}(t)} \\ &= \frac{\int_0^1 (\boldsymbol{\beta}(s, t) - \hat{\boldsymbol{\beta}}_{LM}(s, t))^T \mathbf{V}^{\tilde{\mathbf{X}}}(s)^{-1} \boldsymbol{\Delta}^{\tilde{\mathbf{X}}}(s) ds}{\left(\text{Cov}_{Y_\Delta, Y_i} \left[\int_0^1 \hat{\boldsymbol{\beta}}_{LM}(s, t)^T \mathbf{V}^{\tilde{\mathbf{X}}}(s)^{-1} \mathbf{X}_\Delta ds | \mathbf{X}_\Delta, \mathbf{X}_i \right] + v_\varepsilon^2 \right)^{1/2}} (t). \end{aligned}$$

The latter denominator has been obtained by the following result

$$\begin{aligned} & \text{Cov}_{Y_\Delta, Y_i}(Y_\Delta - \hat{Y}_{LM} | \mathbf{X}_\Delta, \mathbf{X}_i)(t) \\ &= \text{Cov}_{Y_\Delta, Y_i} \left[\int_0^1 \hat{\boldsymbol{\beta}}_{LM}(s, t)^T \mathbf{V}^{\tilde{\mathbf{X}}}(s)^{-1} \mathbf{X}_\Delta ds | \mathbf{X}_\Delta, \mathbf{X}_i \right] (t) + v_\varepsilon^2(t), \quad t \in [0, 1]. \end{aligned}$$

When the truncation parameters L and M and the sample size increase, note that the integral

$$\int_0^1 \left(\boldsymbol{\beta}(s, t) - \hat{\boldsymbol{\beta}}_{LM}(s, t) \right)^T \mathbf{V}^{\tilde{\mathbf{X}}}(s)^{-1} \boldsymbol{\Delta}^{\tilde{\mathbf{X}}}(s) ds$$

converges (in probability) to zero (see Equation (34)); the denominator converges (in probability) to v_ε^2 , because $\text{Cov}_{Y_\Delta, Y_i} \left[\int_0^1 \hat{\boldsymbol{\beta}}_{LM}(s, t)^T \mathbf{V}^{\tilde{\mathbf{X}}}(s)^{-1} \mathbf{X}_\Delta ds | \mathbf{X}_\Delta, \mathbf{X}_i \right]$ converges (in probability) to zero.

Therefore, $E_{Y_\Delta} (e_{stu\Delta} | \mathbf{X}_\Delta, \mathbf{X}_i, Y_i)$ converges (in probability) to zero, as well as $E_{Y_\Delta, Y_i} (e_{stu\Delta} | \mathbf{X}_\Delta, \mathbf{X}_i)$, being the expectation a continuous operator (Casella and Berger, 2002).

F Real-case Study: Plot of Response and Covariate Profile Observations

Figure 4 shows the 315 profiles observed for the covariates and response in the real-case study of Section 5. The functional response is the *cumulative fuel consumption (CFC)* per each voyage. The scale on the ordinate axis is omitted for confidentiality reasons. The covariates are the *sailing time (T)*, measured in hours (*h*) the *speed over ground (SOG)*, measured in knots (*kn*), and the *longitudinal* and *transverse wind components* (W_{lo} and W_{tr}), measured in knots (*kn*).

Figure 4. Plot of the 315 covariate and response observations in the real-case study.

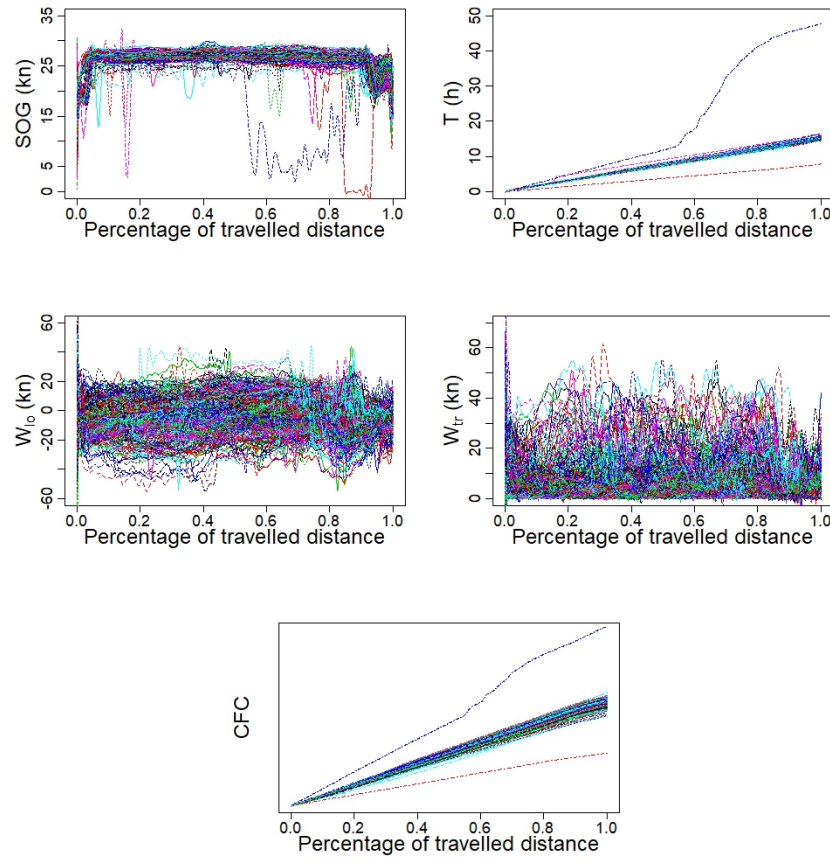
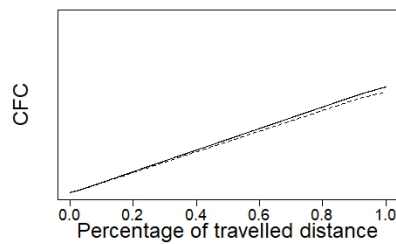


Figure 5 shows the mean function of the response (CFC) before and after the EEI (energy efficiency initiative). By visual inspection, it is clear that a shift downward of the cumulative fuel consumption occurred.

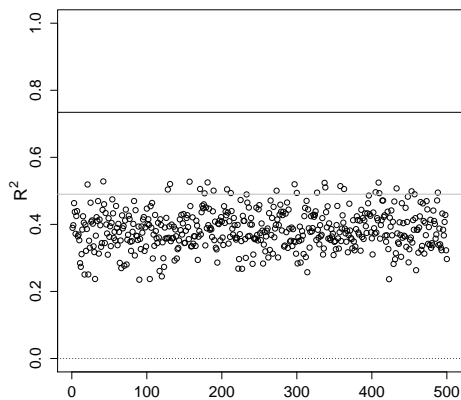
Figure 5. Mean function of the CFC before (solid line) and after (dashed line) the EEI.



G Real-case Study: A Permutation Test to Assess the Statistical Significance of the MFLR Model

We perform a permutation test to assess the statistical significance of the MFLR model estimated as in Section 2 in the real-case study of Section 5. The test is based on $R^2 = \int_{[0,1]} \frac{\text{Var}(E(Y(t)|\mathbf{X}))}{\text{Var}(Y(t))} dt$ (Horváth and Kokoszka, 2012). In Figure 6, the black solid line indicates the observed R^2 that is equal to 0.73. The points represent 500 R^2 values obtained by random permutations of the response variable. Whereas, the grey solid line corresponds to the 95th sample percentile. All of the 500 R^2 values as well as the 95th sample percentile is far below 0.73, and gives a strong justification for the use of the proposed MFLR model.

Figure 6. R^2 values from permuting the response 500 times (points), observed R^2 (black solid horizontal line) and 95th sample percentile (grey solid horizontal line).



H Real-case Study: Bootstrap Analysis Details

Given the n observations in Phase II $(\tilde{\mathbf{X}}_i, \tilde{Y}_i)$, $i = 1, \dots, 203$, of the covariates and response, the bootstrap analysis can be summarized in the following steps.

1. Compute the standardized versions (\mathbf{X}_i, Y_i) of $(\tilde{\mathbf{X}}_i, \tilde{Y}_i)$, using the quantities estimated in Phase I.

2. Obtain B standard bootstrap samples of size n $(\mathbf{X}_{1b}, Y_{1b}), \dots, (\mathbf{X}_{nb}, Y_{nb})$, $b = 1, \dots, B$, resampling with replacement from the standardized observations $(\mathbf{X}_1, Y_1), \dots, (\mathbf{X}_n, Y_n)$.
3. Use the B bootstrap samples $(\mathbf{X}_{1b}, Y_{1b}), \dots, (\mathbf{X}_{nb}, Y_{nb})$, $b = 1, \dots, B$, to compute B values of the statistic, ARL_1, \dots, ARL_B for each chart.
4. Build the confidence interval with confidence level $1 - \alpha$ for the ARL statistics using the $\alpha/2$ and $1 - \alpha/2$ quantiles of the empirical bootstrapped ARL distribution and calculate the mean, \overline{ARL}^* , of the empirical bootstrapped ARL distribution for each control chart.

The number of bootstrap samples B is set equal to 500, and confidence intervals are built with $\alpha = 0.05$.

References

- Abrahamsen, P. and N. Regnesentral (1997). *A Review of Gaussian Random Fields and Correlation Functions*. Norsk Regnesentral/Norwegian Computing Center.
- Abramowitz, M. and I. A. Stegun (1964). *Handbook of mathematical functions: with formulas, graphs, and mathematical tables*. Courier Corporation.
- Casella, G. and R. L. Berger (2002). *Statistical inference*, Volume 2. Duxbury Pacific Grove, CA.
- Horváth, L. and P. Kokoszka (2012). *Inference for functional data with applications*. Springer Science & Business Media.
- Stein, M. (1999). *Interpolation of Spatial Data: Some Theory for Kriging*. Springer New York.
- Yao, F., H.-G. Müller, and J.-L. Wang (2005). Functional data analysis for sparse longitudinal data. *Journal of the American Statistical Association* 100(470), 577–590.